Journal of Surgical Research **162,** 110–121 (2010)
doi:10.1016/j.jss.2009.01.019

Interleukin-17F-Induced Pulmonary Microvascular Endothelial Monolayer Hyperpermeability *Via* the Protein Kinase C Pathway

Qing-hai You, M. Med.,* Geng-yun Sun, M.D.,*,[1] Nan Wang, M. Med.,* Ji-long Shen, Ph.D.,† and Yuan Wang, Ph.D.‡

**Department of Respiratory Medicine, the First Affiliated Hospital of Anhui Medical University, Anhui, Hefei, China; †Key Laboratory of Gene Resource Utilization for Severe Diseases of Ministry of Education, Key Laboratory of Zoonoses (Anhui Medical University), Anhui, Hefei, China; and ‡Laboratory of Molecular Biology, Key Laboratory of Gene Resource Utilization for Genetic Diseases of Ministry of Education and Anhui Province, Anhui, Hefei, China*

Submitted for publication November 5, 2008

Background. **Interleukin (IL)-17F is involved in lung inflammation, but the effect of IL-17F on endothelial permeability and its signaling pathway remain ill-defined. The current study sought to investigate the effect of IL-17F on endothelium and assess the role of protein kinase C (PKC) and src-suppressed C kinase substrate (SSeCKS) in this process.**

Methods. **Rat pulmonary microvascular endothelial monolayers were constructed to determine changes of permeability as measured by means of FITC-dextran and Hank's solution flux across monolayers and trans-endothelial electrical resistance with or without IL-17F and PKC inhibitors. Additional monolayers were stained using FITC-phalloidin for filamentous actin (F-actin). The gene expression of SSeCKS was analyzed by the reverse transcription-polymerase chains. Alterations of SSeCKS protein were investigated by immunoblotting and immunoprecipitation.**

Results. **IL-17F increased endothelial monolayer permeability in a dose- and time-dependent manner. F-actin staining revealed that permeability changes were accompanied by reorganization of cytoskeleton. In the presence of PKC inhibitors, the IL-17F-induced hyperpermeability and reorganization of F-actin were attenuated. The gene and protein expression of SSeCKS were conspicuously elevated after IL-17F challenge. The process of SSeCKS phosphorylation followed a time course that mirrored the time course of hyperpermeability induced by IL-17F. IL-17F-induced SSeCKS phosphorylation was abrogated after PKC inhibitors pretreatment. The translocation of SSeCKS from the cytosol to the membrane and a significant increase in the SSeCKS association with the cytoskeleton were found after IL-17F treatment.**

Conclusions. **IL-17F is an important mediator of increased endothelial permeability. PKC and SSeCKS are integral signaling components essential for IL-17F-induced hyperpermeability.**

Key Words: **rat pulmonary microvascular endothelial cell; interleukin-17F; permeability; protein kinase C; src-suppressed C kinase substrate.**

INTRODUCTION

Interleukin (IL)-17F, a member of the IL-17 cytokine family, is a novel proinflammatory cytokine that is produced by activated $CD4^+$ T cells, human mast cells and basophils [1]. Expression of IL-17F shows a wider tissue distribution than IL-17A, a prototype of the IL-17 family, with marked expression of IL-17F in the human lung, liver, and fetal liver tissue, unlike IL-17A [2]. Accumulating studies have shown that IL-17F triggers a variety of inflammatory responses such as inducing inflammatory factors, including IL-6, IL-8, transforming growth factor-β, and intracellular adhesion molecule-1, in airway epithelial cells, vein endothelial cells, and fibroblasts [1–4]. Of note, in lung, increased expression of IL-17F has been found in animal models after *Klebsiella pneumoniae*, *Mycoplasma pneumoniae,* and *Candida albicans* infection [5–7], and to induce pulmonary neutrophilia and an additive effect on antigen-induced allergic inflammatory responses [8].

[1] To whom correspondence and reprint requests should be addressed at Department of Respiratory Medicine, the First Affiliated Hospital of Anhui Medical University, Ji Xi Road 218, Anhui, Hefei, 230022, China. E-mail: sungengyun@yahoo.com.cn.

0022-4804/$36.00

These findings have suggested that IL-17F is one of the key cytokines regulating the expression of lung inflammation. However, the exact role of IL-17F in lung inflammatory diseases has not been elucidated.

Pulmonary microvascular endothelial cells (PMVECs) localized at the critical interface between the blood and vessel wall present a function of the cellular barrier to regulate tissue fluid balance. As a primary target of inflammatory cytokines, responses of PMVECs to inflammatory cytokines include up-regulation of adhesion molecules, cytoskeletal changes, and permeability increase [9]. Many inflammatory cytokines, such as tumor necrosin factor-α (TNF-α), IL-1β, angiotensin II (Ang II), and so on, act on PMVECs to disrupt the barrier integrity [9–11]. IL-17F can also regulate secretion of inflammatory mediators from PMVECs [12,13]. Yet, little information exists in what changes occur during the IL-17F-induced pulmonary microvascular endothelium injury.

Previous reports have demonstrated that protein kinase C (PKC) pathway significantly contributes to the PMVECs barrier breakdown though phosphorylation of proteins, which can promote cytoskeletal reorganization or dissolution of the adherens junctions [14–16]. In our laboratory, we also have examined the role of PKC, especially PKCδ, in permeability changes of rat PMVECs (RPMVECs) in response to inflammatory mediators, for instance, TNF-α and lipopolysaccharide (LPS). Other reports suggest that activated PKC may control cytoskeletal architecture by dominating over other signaling pathways, such as RhoA and mitogen activated protein kinase (MAPK) [17,18], which involve in the regulation of endothelium permeability [19,20]. Given the complex interplay between PKC pathways and the possible contribution of other signaling pathways, further studies should be required to delineate downstream targets of PKC and the mechanisms by which PKC regulates endothelial barrier function in RPMVECs.

Src-suppressed C kinase substrate (SSeCKS) is a PKC substrate that is identified to regulate inflammation through selective binding of signaling proteins such as PKC, protein kinase A (PKA), calmodulin, cyclin, and β-adrenergic receptor [21–24]. Molecular studies of SSeCKS have revealed biochemical and physical associations with phospholipid-dependent PKC activity [25]. Of particularly interest, evidences that SSeCKS is involved in a dramatic rearrangement of the actin cytoskeleton and the modulation of the blood-brain barrier permeability have been presented [24, 26, 27]. Moreover, in RPMVECs, increased levels of SSeCKS have been found after challenge of LPS [28]. These implicate that SSeCKS is possibly one of the critical protein in the pathogenesis of endothelial hyperpermeability after exposure of PMVECs to various inflammatory factors. Nevertheless, besides LPS, other potential inducers of SSeCKS in RPMVECs remain ill-defined.

Therefore, in the present study, RPMVECs are used to test the hypothesis that IL-17F could disrupt the endothelial cell barrier, and these changes are reflected in PKC signal pathway though alterations of SSeCKS. Furthermore, we also suppose that IL-17F and signal pathways activated by IL-17F could lead to actin cytoskeleton changes that contribute to endothelial permeability.

MATERIALS AND METHODS

Materials

Recombinant rat IL-17F was obtained from R and D Systems (Minneapolis, MN). Bisindolylmaleimide I (BIM) was from Calbiochem (La Jolla, CA). Rottlerin was from ALEXIS Biochemicals (San Diego, CA). Horseradish peroxidase (HRP)-labeled antibody to sheep IgG was purchased from KPL (Gaithersburg, MD). Polyclonal anti-SSeCKS antibody, fluorescein isothiocyanate (FITC)-conjugated *Bandeiraea simplicifolia* I isolectin B4 (BSI), FITC-labeled dextran, unlabeled dextran and FITC-conjugated phalloidin were all purchased from Sigma (St. Louis, MO). Trizol isolation reagent and reverse transcription system were obtained from Promega (Madison, WI). High glucose Dulbecco's modified Eagle's medium (DMEM) was purchased from Invitrogen (Carlsbad, CA). Fetal calf serum, penicillin, streptomycin, and trypsin were purchased from HyClone Laboratory (Salt Lake City, UT).

Endothelial Cell Culture

Isolation and culture of RPMVECs were performed according to a method developed by Chen SF *et al.* and modified by Zhang H *et al.* [10, 29, 30]. Briefly, following the pleura and the outer edges of the aseptically fresh rat lung were cut off, the tissues of the lung surface were cut into pieces, and plated as explants into culture flasks. The small tissue pinches were fed on the culture medium containing DMEM, 20% fetal calf serum, 100 U/mL penicillin, 0.1 mg/mL streptomycin and 15 μg/mL endothelial cell growth supplement (Upstate Biotechnology, Lake Placid, NY), and incubated in 5% CO_2 plus humidified air at 37 °C. After 60 h, the residue lung tissues were removed. When a contact-inhibited monolayer was achieved, RPMVECs were harvested. Cells were identified according to (1) the characteristic "cobble-stone" appearance, (2) the presence of staining with anti-human factor VIII related-antigen, (3) the binding of lectin BSI [29, 31, 32]. Experimental data were obtained from cells in their third to fifth passages.

Binding of Lectin BSI and Immunocytochemical Staining

Primary RPMVECs were seeded onto sterile poly-L-lysine-coated coverslips and allowed to grow for 3 to 6 h. After fixation using acetone, the cells were incubated with FITC-conjugated BSI (25 μg/mL), and observed under a fluorescence microscope (Olympus IX-71; Olympus Co., Tokyo, Japan). For immunocytochemical staining, after fixed cells were incubated with 100% methanol containing 3% H_2O_2 and blocked with 10% goat serum, they were reacted with rabbit anti-human factor VIII related-antigen antibody (1:100; Boster Biological Technology Ltd., Wuhan, China), then incubated with biotinylated anti-rabbit IgG (1:200), and visualized by exposure of the cells to a streptavidin biotin-peroxidase complex and a solution of 3, 3'-diaminobenzidine-4-HCl. After hematoxylin was applied for nuclear counterstaining, the coverslips were subsequently drained, dehydrated, and viewed.

Measurement of the Endothelial Cell Monolayer Permeability

Permeability was determined following the published method with some modification [33, 34]. To construct an in vitro model of RPMVECs monolayer, a cell suspension (1×10^5 cells/cm^2) was cultured on gelatin-coated polyester filters (0.4-μm pore size; Transwell, 12-well type; Costar, Cambridge, MA). The transendothelial electrical resistance (TER, $\Omega \cdot cm^2$) was measured daily with an epithelial volt-ohmmeter and STX-2 electrodes (EVOM; World Precision Instruments, Sarasota, FL) according to the manufacturer's protocol. Once stable resistances were obtained, fresh serum-free media were applied, and the resistances were allowed to stabilize for 24 h. At the end of stimulations, besides measurement of TER, the transendothelial flux of FITC-labeled dextran with average molecular weight of 10 kDa was used to evaluate the status of RPMVECs monolayers [33]. Briefly, after stimulations, the top chamber was replaced with fresh phenol red-free DMEM containing FITC-labeled dextran (500 μg/mL), and incubated for 1 h at 37 °C. To maintain isotonic condition, an equimolar amount of unlabelled dextran mixed with phenol red-free DMEM was added to the bottom chamber. Sample was collected from sides of the filter for analysis using a fluorescent microplate reader. The permeability coefficient (P_d, cm/s), based on the flux of FITC-labeled dextran across the monolayer, was calculated according to the following equation: $P_d = ([A]/t) \times (1/A) \times (V/[L])$, where [A] is bottom concentration, t is time in s, A is area of membrane in cm^2, V is volume of bottom chamber, and [L] is top concentration [15].

In our laboratory, RPMVECs were also cultured on a specially pretreated round polycarbonate filter membrane (12-mm diameter, 0.45-μm pore size). Diffusion of Hank's buffer solution across the confluent monolayer was performed to assess the endothelial barrier function using a modified protocol [10, 34]. Briefly, after stimulation, the membrane containing the endothelial monolayer was sealed between two pieces of polycarbonate assembly separating the top and bottom compartments. The top compartment was fully filled with Hank's buffer solution, which was incubated under constant conditions at 37 °C. The amounts of Hank's solution that permeated the monolayer into the bottom compartment were determined by assay of the removed solution weight during the interval of 10 to 15 min. The fluid permeability coefficient (K_f, cm/s/cm H_2O) was calculated according to the Starling's equation: $J_v = K_f \cdot (\Delta P - \sigma d \cdot \Delta\pi)$. In our experiment, $\Delta\pi$ was 0, the K_f was measured by the converted formula: $K_f = J_v/\Delta P$. Here J_v is the fluid filtration flux across the RPMVECs monolayer, and ΔP represents hydraulic pressures on the monolayer [10, 34].

Fluorescent Staining

After confluent monolayers were fixed, permeabilized, and blocked, incubation was performed with FITC-phalloidin (10 μg/mL) for 1 h at 37 °C to visualize filamentous actin (F-actin) using a fluorescence microscope indicated above. Quantification of F-actin was measured by flow cytometric analysis. Briefly, after confluent RPMVECs were trypsinized, fixed, and permeabilized, they were resuspended in 0.5 mL solution of FITC-phalloidin (1 μg/mL), incubated for 40 min and analyzed by an EPICS XL-MCL flow cytometer using a logarithmic scale (Beckman Coulter, Fullerton, CA). Levels of F-actin were expressed as relative fluorescence intensity and mean fluorescence intensity.

Reverse Transcription-Polymerase Chains Reaction (RT-PCR)

Total RNA was extracted from RPMVECs with Trizol isolation reagent. Reverse transcription was performed according to the manufacturer's protocol, and subjected to PCR. The primers of PCR were as follows: SSeCKS (GenBank accession no. AY695056): 5'-AATC CATCCCAATCATAGTAAC-3' (forward), 5'-TCTCAAGGTCCCAAC AGC-3' (reverse), product is 842 bp. Control β-actin: 5'-ATCCATCC CAATCATAGTAAC-3' (forward), 5'-CTCAAGGTCCCAACAGC-3' (reverse), product is 248 bp. The cycling conditions were performed for 30 cycles with denaturation at 95 °C for 1 min, annealing at 52 °C for 1 min, and extension at 72 °C for 1 min. PCR products were electrophoresed and visualized.

Western Blotting

Confluent RPMVECs were harvested in an ice-cold lysis buffer (25 mM Tris·HCl, pH 7.4, 5 mM EDTA, 100 mM sodium fluoride, 2 mM sodium vanadate, 10 mM sodium pyrophosphate, and 1% Igepal CA-630, Sigma, St. Louis, MO). Cell lysates were centrifuged at 12,000 g for 10 min at 4 °C. After the supernatant protein was normalized, equal volumes of samples were separated by gradient sodium dodecyl sulfate-8% polyacrylamide gel electrophoresis (SDS-PAGE) and transferred onto nitrocellulose membranes. They were subsequently reacted with 1 μg/mL SSeCKS antibody and HRP-conjugated anti-sheep IgG (1:20000). The blots were developed with enhanced chemiluminescence, quantified by densitometry, and estimated by comparison with β-actin.

Immunoprecipitation

Cells were lysed by an extraction buffer (20 mM Tris, pH 7.5, 150 mM NaCl, 1 mM EDTA, 1 mM EGTA, 1% Triton X-100, 2.5 mM sodium pyrophosphate, 1 mM β-glycerophosphate, 1 mM Na_3VO_4, 1 μg/mL leupeptin), and sonicated. Cell lysates were cleared by centrifuging at 14,000 g for 10 min at 4 °C. Protein content was normalized using protein assay kit (Bio-Rad Laboratories, Hercules, CA). After the supernatant was incubated overnight at 4 °C with 1:250 dilutions of the primary antibody, Protein A/G Agarose (Beyotime Institute of Biotechnology, Haimen, China) was added, and incubated for additional 4 h at 4 °C. After washing, the immune complexes were boiled in SDS sample buffer. These samples were subjected to immunoblotting with anti-phospho-Ser PKC substrate antibody (Cell Signaling Technology Inc. Beverly, MA) and SSeCKS antibody according to the manufacture's instructions, respectively.

Analysis of SSeCKS Association with the Actin Cytoskeleton

A Triton X-100 extraction assay as previously described was used to monitor the SSeCKS association with the actin cytoskeleton [35]. RPMVECs were lysed with a buffer containing 1% Triton X-100, 20 mM Tris, pH 7.4, 5 mM EGTA, 20 mM sodium fluoride, 25 mM sodium pyrophosphate, 10 mM dithiothreitol, 0.5 mM phenylmethylsulfonyl fluoride, 0.002% leupeptin, and 0.002% aprotinin. Both soluble and insoluble fractions were clarified by centrifugation at 14,000 g at 4 °C for 1 h, and the proteins were probed with SSeCKS antibody. Data were expressed as a percentage of total SSeCKS in Triton-insoluble fraction.

Analysis of SSeCKS Translocation between Cytosol and Membrane

Cells were pooled into an extraction buffer (20 mM Tris, pH 7.4, 1 mM EDTA, 330 mM sucrose, 100 mM sodium fluoride, 2 mM sodium orthovanadate, 10 mM sodium pyrophosphate, and 0.5 mM phenylmethylsulfonyl fluoride), then sonicated. The supernatants (cytosolic fraction) and the pellets (membrane fraction) were collected by ultracentrifugation at 100,000 g for 1 h at 4 °C, then 10% trichloroacetic acid was added into the supernatants to precipitate the proteins. Both the cytosolic fraction and the membrane fraction were loaded on 8% SDS-PAGE and levels of SSeCKS in each fraction were determined by Western blotting [36].

Data Analysis

All data were expressed as means ± SD. One-way ANOVA followed by t-test was used to examine the differences between more than two groups. $P < 0.05$ was considered statistically significant.

RESULTS

RPMVECs Characteristics

The primary RPMVECs and the subcultured cells grown on dish gave capillary-like structure and typical cobble-stone morphology at confluence (Fig. 1A and B). According to Laitinen [32], the fluorescently conjugated lectin BSI binds primarily to microvascular endothelial cells and does not bind to large vessel endothelial cells or most other control nonendothelial cells. Figure 1C showed that RPMVECs bound FITC-conjugated BSI and displayed positive staining by lectin BSI. Meanwhile, these cells were also characterized as endothelial cells by factor VIII-related antigen expression (Fig. 1D).

IL-17F-Induced Hyperpermeability Across RPMVECs Monolayers

Figure 2A showed that before confluence the normalized TER increased steadily (increase in integrity), beginning at 0 and leveling off at $49.5 \pm 2.4\ \Omega \cdot cm^2$. This was accompanied by the confluence of cells on the fifth d post-seeding (Fig. 2B and C). The effect of IL-17F on the confluent RPMVECs monolayer was determined by measuring changes of P_d, K_f, and TER concurrently. As seen in Fig. 3A, IL-17F induced, in a dose-dependent manner, significant increases of P_d after monolayers were exposed to stimulation for 3 h. Figure 3B demonstrated that the effect of IL-17F was also time dependent. P_d increased ~15% compared with basal levels after monolayers were treated by a fixed concentration of IL-17F (100 ng/mL) for 0.5 h, peaked at 3 h point, and prolonged lag time of 24 h. In experiments of the fluid permeability coefficient to Hanks' buffer solution, significant changes of K_f were observed after IL-17F (range 1–100 ng/mL) challenge for 3 h (Fig. 3C). Figure 3D showed that K_f was increased beginning at 0.5 h point after stimulation with 100 ng/mL IL-17F, peaking at 3 h point, and increased K_f did not return to baseline levels after 24 h of exposure.

Although the transendothelial flux of FITC-dextran or Hank's buffer solution was widely used as a measure of monolayer integrity, they did not readily afford the opportunity to observe barrier status as a function of time. However, the instantaneous data obtained by measuring TER allowed for a more comprehensive time course study. In Fig. 3E, the TER following exposure to multiple concentrations of IL-17F (0.1, 1, 10, and 100 ng/mL) was measured at various periods of time as indicated. The progressive decrease in TER (increase in permeability) produced by IL-17F was statistically significant within 6 h compared with untreated

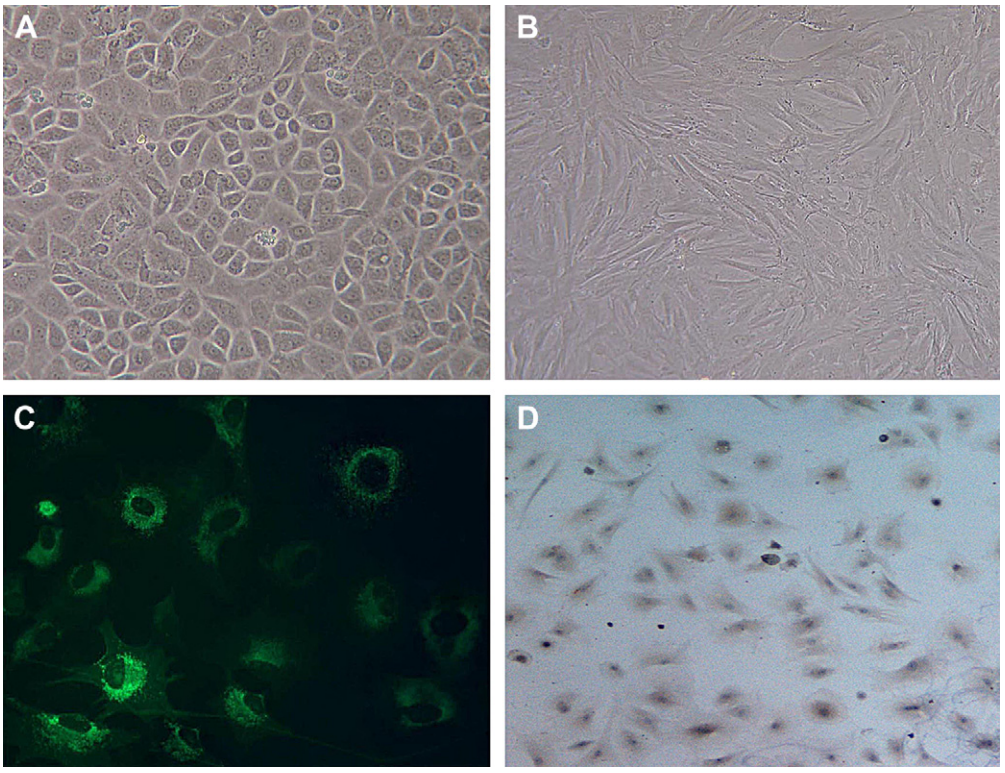

FIG. 1. RPMVECs morphology, binding of Lectin BSI, and staining with anti-human factor VIII related-antigen. Normal primary RPMVECs morphology (A) and sub-cultured RPMVECs morphology (B) were observed under phase-contrast microscopy (magnification ×100). RPMVECs bound to FITC-conjugated BSI under fluorescence microscopy (magnification ×400) (C). Positive expression of factor VIII related-antigen in RPMVECs was demonstrated brown particles in the cytoplasm by immunocytochemical staining (magnification ×100) (D). (Color version of figure is available online.)

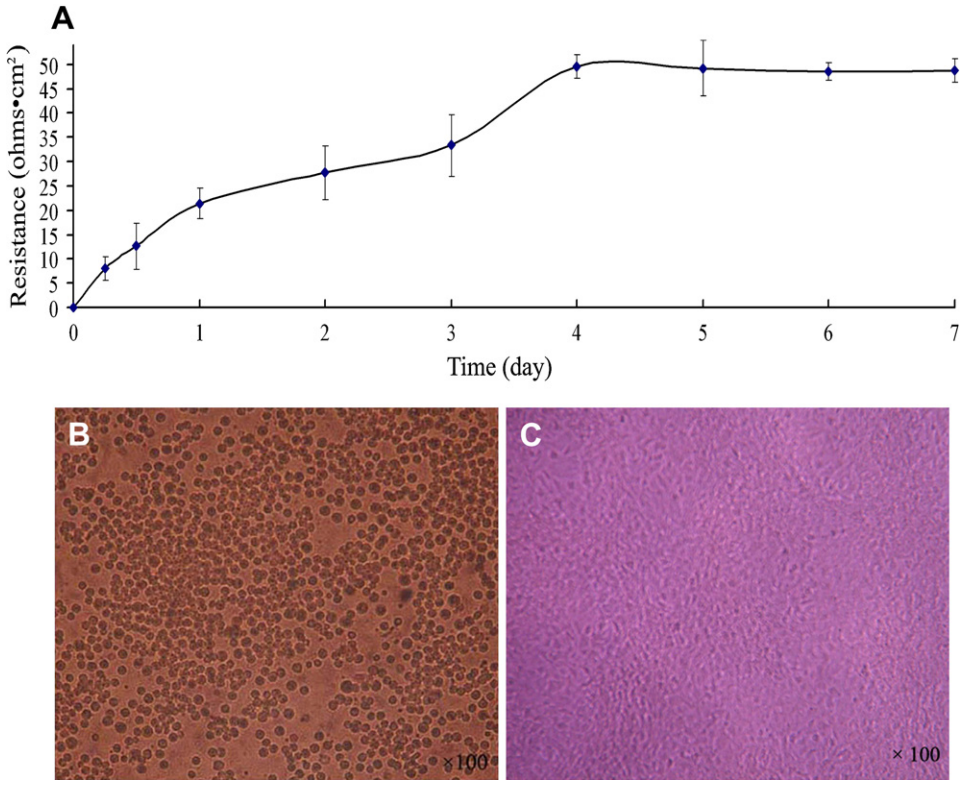

FIG. 2. Development of the normalized TER in RPMVECs monolayers cultured on a Transwell filter. (A) The normalized TER increased steadily, beginning at 0 $\Omega \cdot cm^2$ and leveling off at the maximum on the fifth day ($n = 6$). This was accompanied by the confluence of cells (B) and (C). (Color version of figure is available online.)

monolayers, was sustained over 24 h, and was dose dependent.

PKC-Dependent IL-17F-Induced Hyperpermeability Across RPMVECs Monolayers

To determine whether PKC signal pathway was responsible for IL-17F-induced hyperpermeability, BIM, a general PKC inhibitor was employed in combination with IL-17F. Our preliminary data have identified PKCδ as being required for LPS-induced PKC activity and hyperpermeability in RPMVECs, therefore, Rottlerin (an inhibitor relatively specific for PKCδ) was also used. As expected, none of these inhibitors themselves had a significant effect on basal permeability. After RPMVECs monolayers were pretreated for 30 min with these inhibitors, BIM at 10 μM and Rottlerin at 5 μM, the permeability increase elicited by IL-17F can be significantly blocked (Fig. 4A, B, and C), but increased P_d, K_f, and decreased TER induced by IL-17F did not return to baseline levels.

PKC-Dependent IL-17F-Induced Cytoskeletal Changes of RPMVECs

To assess whether cytoskeletal changes existed in IL-17F-induced RPMVECs, cells were stained with FITC-phalloidin to detect F-actin. We did not serum-starve our cells before staining, as serum starvation resulted in an artificially reduced amount of stress fibers. Therefore, a few centrally located stress fibers were present. As shown in Fig. 5A, untreated monolayers showed strong intercellular connections with F-actin arranged primarily at the periphery; in contrast, IL-17F produced numerous intercellular gaps and a marked reorganization of F-actin from a web-like peripheral distribution to centrally located parallel stress fibers. The latter became thicker (Fig. 5B). We further assessed whether IL-17F-induced cytoskeletal changes correlated with PKC. After monolayers were pretreated with BIM and Rottlerin, IL-17F-induced morphology of F-actin was relatively unchanged compared with control monolayers (Fig. 5C and D). Similarly, the flow cytometric profile was shifted to the right after IL-17F stimulation, indicating that the stimulation induced the formation of F-actin, and returned to the left after BIM and Rottlerin pretreatment (Fig. 5E). Quantitative analysis also showed that IL-17F conspicuously elevated the formation of F-actin, and PKC inhibitors significantly decreased the effect in RPMVECs (Fig. 5F). BIM and Rottlerin themselves had no effect on the F-actin cytoskeletal reorganization (data not shown).

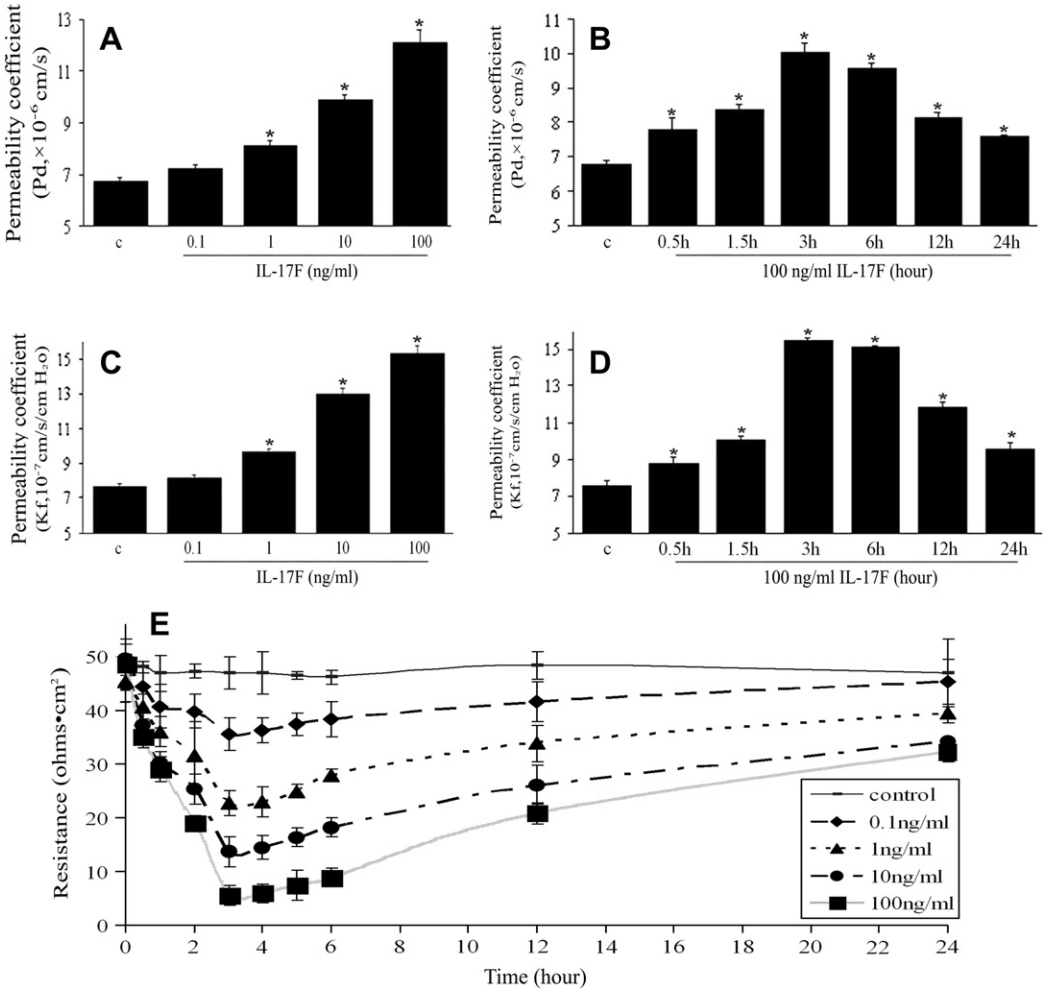

FIG. 3. Effects of IL-17F on RPMVECs monolayers permeability. *$P < 0.01$ *versus* control ($n = 4$). (A) Dose response. After increasing concentrations of IL-17F were incubated with confluent RPMVECs monolayers for 3 h, the permeability coefficient in FITC-dextran flux across monolayers (P_d) was determined. (B) Time response. IL-17F (100 ng/mL) was incubated for increasing exposure times and P_d was measured. RPMVECs monolayers grown to confluence on polycarbonate filter membrane were exposed to IL-17F in a dose- and time-dependent manner, and the permeability coefficient in Hank's buffer solution flux across monolayers (K_f) was shown as dose response (C) and time response (D). (E) At the indicated time points, the TER across confluent RPMVECs monolayers following exposure to multiple concentrations of IL-17F (0.1, 1, 10, and 100 ng/mL) was shown over 24 h period.

IL-17F-Induced Expression of SSeCKS Gene and Protein

Next we investigated whether IL-17F induced the expression of SSeCKS. Cells were treated with increasing concentrations of IL-17F for 3 h and with 100 ng/mL IL-17F for various times. We found that IL-17F led to remarkably up-regulate the expression of SSeCKS gene in a dose- and time-dependence as shown in Fig. 6A and B. Furthermore, the expression of SSeCKS mRNA occurred maximally at 3 h point poststimulation. To confirm whether the protein increase was associated with the elevation of SSeCKS mRNA after IL-17F stimulation, immunoblotting was performed. Fig. 7A and B show that the changes of protein were similar in extent to that of the SSeCKS mRNA in a dose- and time-dependent manner despite few hours later than the peak of the SSeCKS mRNA. One hundred ng/mL IL-17F up-regulated protein expression with a peak at 6 h of stimulation, and slightly increased the level of SSeCKS protein at 24 h following IL-17F treatment (Fig. 7B).

IL-17F-Induced Functional Alterations of SSeCKS Protein

To date, the downstream signaling event of PKC pathway remains unclear. In this research, we investigated some functional alterations of SSeCKS protein to study the mechanisms involved in IL-17F-induced hyperpermeability in RPMVECs. Confluent cells were treated with IL-17F (100 ng/mL) for indicated time. First, we investigated whether IL-17F was able to induce the phosphorylation of SSeCKS in RPMVECs. The results showed that the phosphorylation of SSeCKS

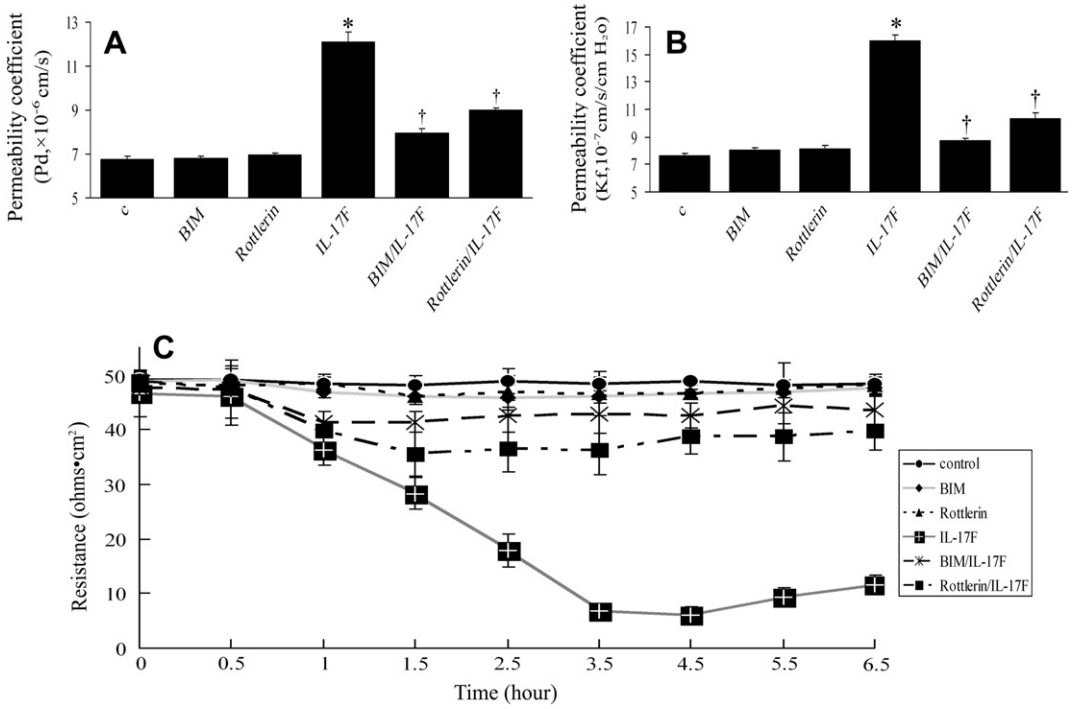

FIG. 4. Effects of PKC inhibitors on IL-17F-induced RPMVECs monolayers hyperpermeability. Confluent RPMVECs monolayers were pretreated with bisindolylmaleimide I (BIM, 10 μmol/L) and Rottlerin (5 μmol/L) for 30 min, followed by IL-17F (100 ng/mL) for 3 or 6 h. The P_d (A), K_f (B), and TER (C) were evaluated as described in METHODS ($n = 4$). *$P < 0.01$ *versus* control, †$P < 0.01$ *versus* IL-17F.

protein was weakly detected after 5 min stimulation, and remarkably occurred at the 30 min point poststimulation. IL-17F-induced SSeCKS protein phosphorylation reached maximal level at 3 to 6 h poststimulation, and stayed at a slightly high level until 24 h after exposure (Fig. 8A). Our findings also showed that preincubation of cells with BIM and Rottlerin significantly abrogated this phosphorylation induced by IL-17F for 3 h (Fig. 8B). Second, it is well known that SSeCKS is an actin-binding protein in a phosphatidylserine-dependent manner, and F-actin in nonmuscle cells is resistant to Triton solubilization, whereas globular actin is soluble in Triton [24, 26]. Thus, alterations in Triton-insoluble actin represent the amount of actin-binding protein and F-actin assembled in the cytoskeleton. Our result demonstrated that treatment with IL-17F significantly increased the amount of SSeCKS in the insoluble fraction in a time-dependent manner (Fig. 9). Finally, under certain conditions in some cell types, SSeCKS is translocated from the cytosol to the membrane on phosphorylation [24, 28]. As shown in Fig. 10, under basal conditions in RPMVECs, SSeCKS existed for the most part in the cytosolic fraction. After 30 min of treatment, IL-17F resulted in significant translocation of SSeCKS from the cytosol to the membrane. At 90 min point, SSeCKS predominantly existed in the membrane fraction. Since synthesis of the protein significantly increased after 90 min, the evaluation of SSeCKS translocation was not performed in our date.

DISCUSSION

These findings have clearly demonstrated the following: (1) IL-17F causes barrier dysfunction in cultured RPMVECs monolayers. (2) PKC plays an important role in the regulation of both functions, i.e., the hyperpermeability and the formation of F-actin, in IL-17F-induced RPMVECs. (3) SSeCKS is required for IL-17F and PKC signal cascade in RPMVECs.

Failure of pulmonary microvascular endothelial barrier function, the hallmark of inflammatory diseases such as the acute respiratory distress syndrome, occurs when endothelial cells are exposed to inflammatory mediators. Our three established indices of barrier function provide direct evidence that IL-17F can cause RPMVECs monolayer hyperpermeability injury. As a novel proinflammatory cytokine in response to pathogenic bacterium infection in lung [5–7], the effect of IL-17F on endothelial permeability found in this study is consistent with the effects of other inflammatory cytokines such as TNF-α, IL-1β, and Ang II [9, 10], together with other roles of IL-17F in lung, such as inducing the release of proinflammatory and neutrophil-mobilizing cytokines, then infiltration of lymphocytes and macrophages, and mucus hyperplasia [37], we propose that IL-17F could play a vital role in the pulmonary inflammatory process.

To assess the barrier dysfunction induced by IL-17F, we have constructed a cultured RPMVECs monolayer

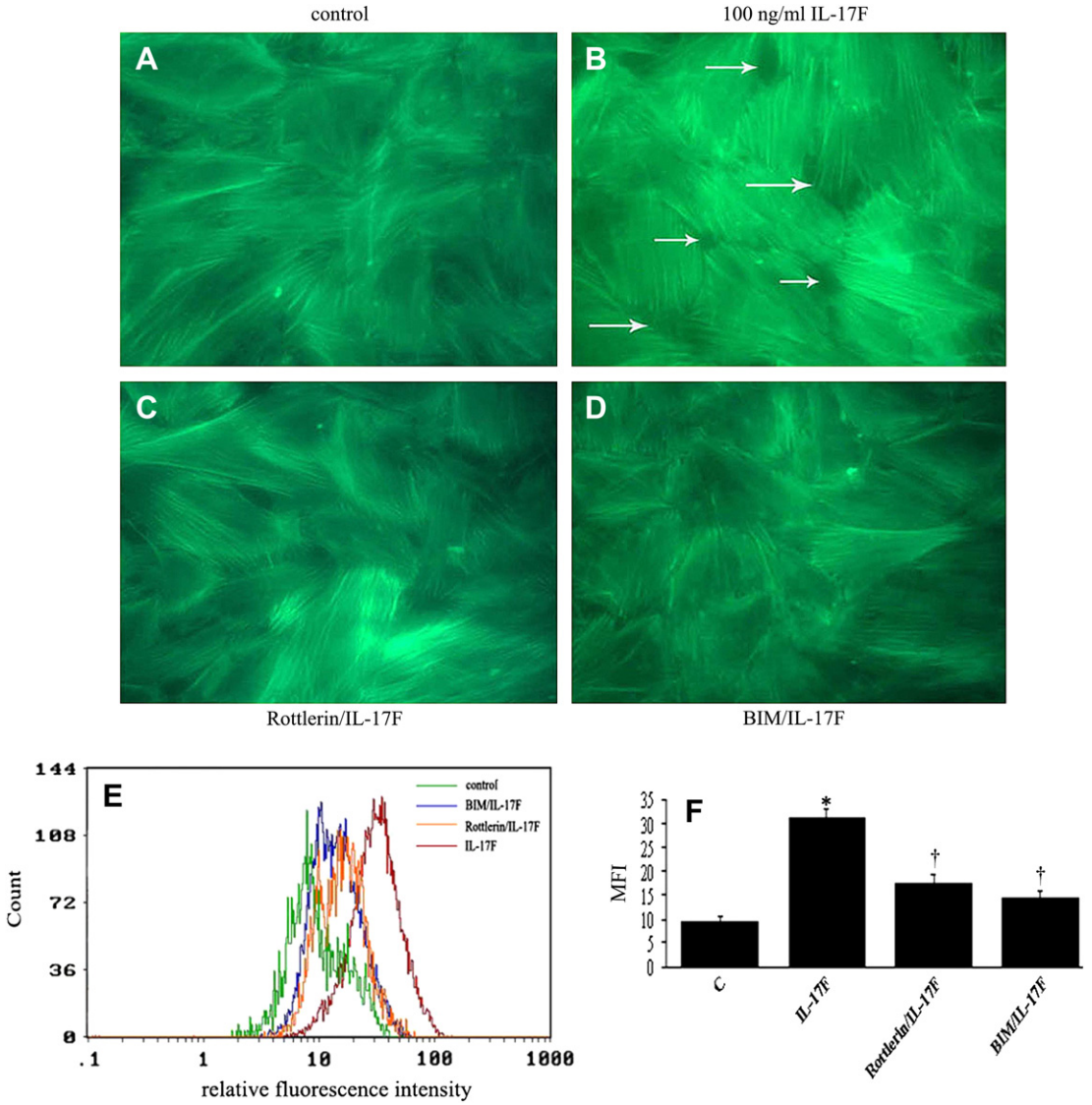

FIG. 5. Effects of IL-17F and PKC inhibitors on RPMVECs actin cytoskeletal organization. A representative image of cellular F-actin among four experiments was shown using a fluorescence microscope (magnification ×400). (A) Control monolayers. (B) IL-17F-induced endothelial cells had abundant actin stress fibers and numerous intercellular gaps (arrows). For effects of Rottlerin (C) and BIM (D) on IL-17F-induced actin cytoskeletal reorganization, monolayers were pretreated with BIM (10 μmol/L) and Rottlerin (5 μmol/L) for 30 min, followed by 100 ng/mL IL-17F for 3 h. After confluent RPMVECs were fixed and stained with FITC-phalloidin, F-actin was quantitated using flow cytometric analysis ($n = 4$). (E) Representative flow cytometric profiles of RPMVECs stimulated with or without drugs. (F) Levels of F-actin were analyzed by the mean fluorescence intensity (MFI). *$P < 0.01$ *versus* control, $^{\dagger}P < 0.01$ *versus* IL-17F. (Color version of figure is available online.)

with the use of the same Transwell culture system, identical filter pretreatment, and similar culture duration. Furthermore, before confluence, TER measurements have been employed to evaluate the integrity of cellular junction, therefore the consistency of the results as well as the ease of manipulation can be identified. Owing to the effective concentrations of IL-17F experimentally determined in cell culture of RPMVECs, of between 0.1 and 100 ng/mL, this concentration range being comparable to both the results of methyl thiazolyl tetrazolium assay (data not shown) and other reports [5–7, 37–39], we believe that exogenous IL-17F alone certainly has injury effect on normal PMVECs barrier.

It is generally believed that in response to inflammatory cytokines, changes in endothelial permeability have been associated with reorganization of the actin cytoskeleton [40–42]. In the current study, fluorescence staining for F-actin has demonstrated that the functional permeability changes induced by IL-17F are accompanied by morphological changes including actin reorganization from a peripheral distribution to centrally located stress fibers, a marked enhancement of polymerized F-actin, and the appearance of intercellular gaps. Collectively, our findings also support a cytoskeletal mechanism for the permeability changes resulting from IL-17F exposure and agree

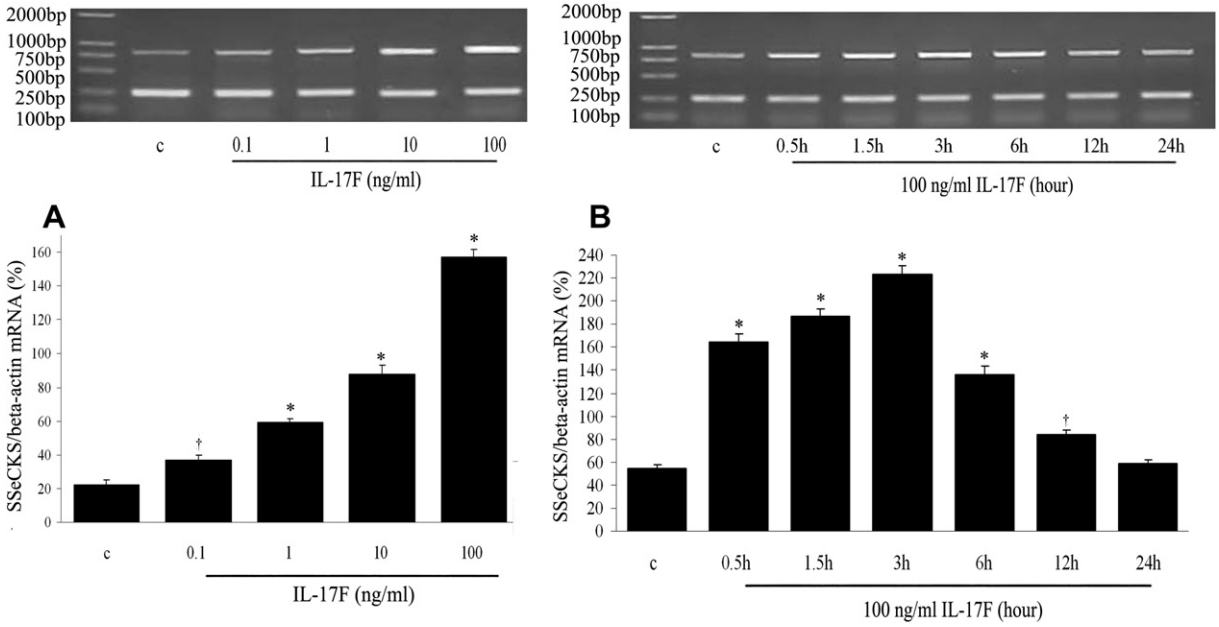

FIG. 6. IL-17F induced SSeCKS mRNA expression in RPMVECs. Cells were treated by increasing concentrations of IL-17F for 3 h (A), a fixed concentration of IL-17F (100 ng/mL), or media alone for increasing exposure times (B). $^{\dagger}P < 0.05$ and $^{*}P < 0.01$ *versus* control. Representative PCR blots are shown above the bar graphs ($n = 4$).

with other studies emphasizing the importance of cytoskeletal actin in endothelial barrier function [40–42].

A multitude of signaling pathways have been implicated in the regulation of PMVECs barrier function and actin cytoskeleton [14–16, 40–42]. Especially, the PKC signal pathway has been widely established to play an important role in these processes. For instance, PKC was involved in the hyperpermeability induced by phorbol 12-myristate 13-acetate (PMA) and TNF-α-induced actin cytoskeletal changes in RPMVECs [14, 16]. In this study, we also have found a significant salutary effect of PKC inhibitor on IL-17F-induced hyperpermeability and the formation of F-actin, but the effect of PKC inhibitor is not complete in RPMVECs, just partly. Several factors could account for the phenomena. One is that five isoforms of PKC (α, βI, δ, ϵ, and PKD) are present in RPMVECs, and different isoforms of PKC may exhibit various and possibly opposing effects [16]. Another is that other signaling pathways such as MAPK and protein tyrosine kinase maybe mediate IL-17F-induced signaling events in RPMVECs [11, 14, 38]. In addition, the attenuation of the PKC inhibitor is also dosage-dependent [15]. However, the current study, for the first time, demonstrates that IL-17F-induced PMVECs barrier injury

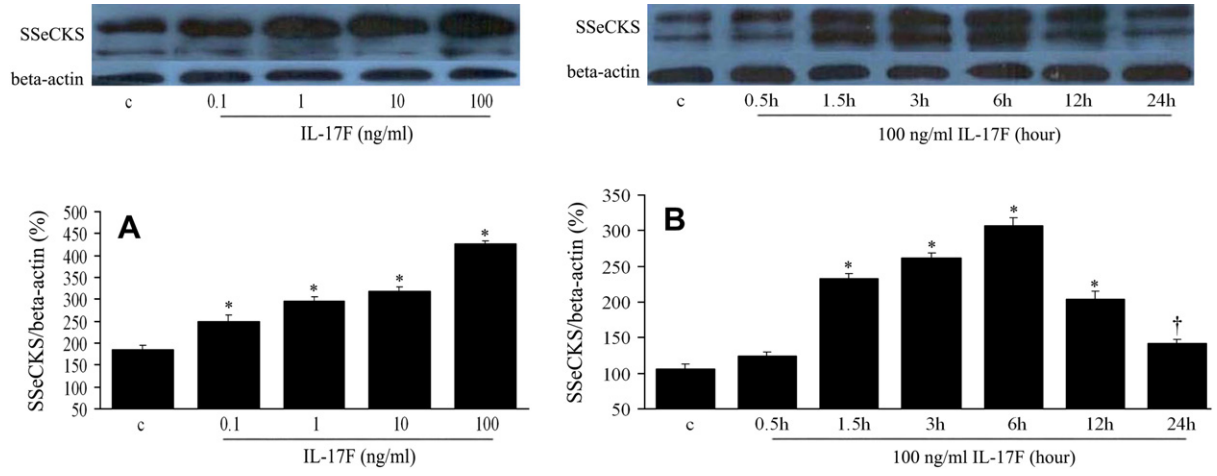

FIG. 7. IL-17F induced SSeCKS protein expression in RPMVECs. Cells were treated by increasing concentrations of IL-17F for 6 h (A), a fixed concentration of IL-17F (100 ng/mL), or media alone for increasing exposure times (B). $^{\dagger}P < 0.05$ and $^{*}P < 0.01$ *versus* control. Representative Western blots are shown above the bar graphs ($n = 4$). (Color version of figure is available online.)

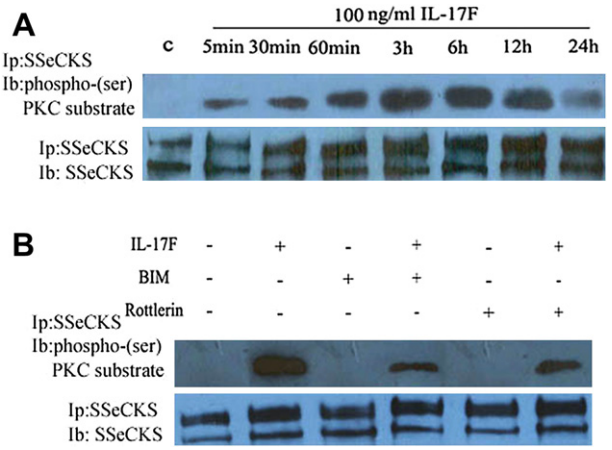

FIG. 8. IL-17F induced SSeCKS phosphorylation. (A) Confluent RPMVECs were treated with IL-17F (100 ng/mL) for indicated time. (B) RPMVECs were pretreated with BIM (10 μmol/L) or Rottlerin (5 μmol/L) for 30 min, followed by IL-17F (100 ng/mL) treatment for 3 h. SSeCKS was immunoprecipitated (Ip) and the pellets subjected to immunoblotting (Ib) with antibody against phosphoserine (top bots). Bottom blots demonstrated equal loading of protein by detecting SSeCKS ($n = 4$). (Color version of figure is available online.)

and reorganization of the actin cytoskeleton at least occur partly via the PKC signal pathway.

Although activation of PKC induced by IL-17F in RPMVECs can result in cytoskeletal reorganization associated with hyperpermeability, the downstream molecular mechanisms are not well understood. Previous studies have reported that myristoylated alanine-rich C kinase substrate, a PKC substrate, was closely linked to hyperpermeability induced by PMA and diacylglycerol in RPMVECs [16]. In our study, we have provided new evidence showing that IL-17F can up-regulate the mRNA and protein expression of SSeCKS, a novel PKC substrate working at the junction of PKC signaling and cytoskeletal control pathways. These results obtained are consistent with the findings in reoxygenation-induced astrocyte and LPS-induced RPMVECs [27, 28], and support our hypothesis that IL-17F is one of the key inducers of SSeCKS in RPMVECs. According to some previous reports, the abundance of SSeCKS protein could affect actin organization [24, 26, 28, 43], even permeability modulation [27]. The above results and considerations indicate that the IL-17F-induced increase in levels of SSeCKS protein may contribute to the roles of PKC in the IL-17F-induced RPMVECs hyperpermeability and actin reorganization. Of particular interest is that IL-17F, TNF-α, and Ang II, which were endogenous humoral factors stimulated by LPS, might participate in SSeCKS induction [44, 45], but no increase of SSeCKS mRNA and protein was detected after LPS stimulation in mouse endothelial cell line LEII [44], and the change of SSeCKS mRNA levels occurred earlier and was more pronounced than the corresponding changes of SSeCKS protein levels in rat aortic smooth muscle cells [45]. The controversial findings indicate that endothelial cells from different sites, tissues, and species can respond differently to inflammatory stimuli. Alternatively, the stimuli induction of SSeCKS mRNA levels in cells may mainly result in post-translational alterations of the protein, such as phosphorylation-state changes [46, 47].

Most importantly with regard to our work, this study has strongly suggested that stimulation of RPMVECs by IL-17F can result in a rapid serine phosphorylation of SSeCKS, and this phosphorylation can be partly abrogated in the presence of PKC inhibitors, which is consistent with the previous results of SSeCKS phosphorylation induced by PMA in mesangial cells [43]. The process of phosphorylation follows a time course that closely mirrors the time course of hyperpermeability induced by IL-17F, along with other reports that changes of SSeCKS phosphorylation levels could affect actin organization [24, 26, 43]; we may believe that a marked increase in PKC-dependent phosphorylation of SSeCKS is required for RPMVECs permeability injury induced by IL-17F. In addition, it is well known that some functions of SSeCKS, including the binding with F-actin and translocation, are regulated by PKC phosphorylation [24, 28, 48]. In our study, the translocation of SSeCKS from the cytoplasm to the membrane and the increased SSeCKS in the actin cytoskeleton have been found after IL-17F stimulation, and the time course is similar in extent to the process of SSeCKS phosphorylation induced by IL-17F, indicating that they may together contribute to cytoskeletal reorganization and cell shape change required for IL-17F-induced endothelial hyperpermeability.

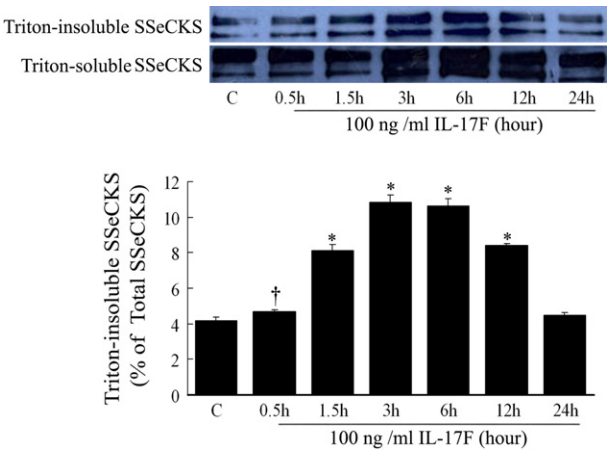

FIG. 9. SSeCKS association with actin cytoskeleton in IL-17F-induced RPMVECs. SSeCKS associated with the Triton-insoluble (cytoskeletal) fraction were quantified as described in METHODS ($n = 4$). Shown above the bar graphs are representative Western blots in which 20% of the Triton-insoluble fraction and 5% of the Triton-soluble fraction were used. $^{\dagger}P < 0.05$ and $^{*}P < 0.01$ *versus* control. (Color version of figure is available online.)

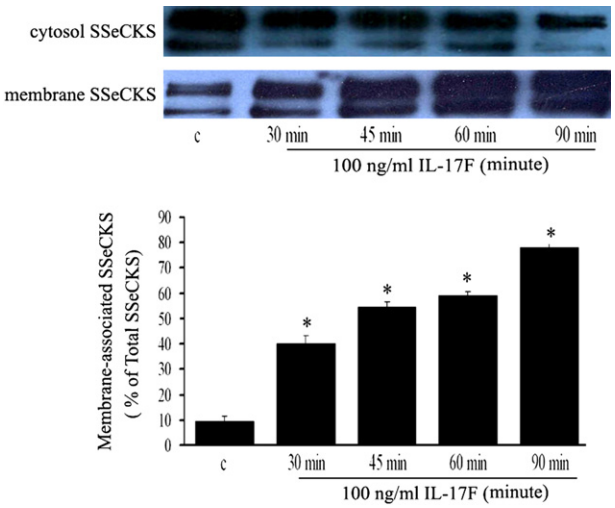

FIG. 10. IL-17F induced SSeCKS translocation between cytosol and membrane in RPMVECs. After confluent RPMVECs were treated with IL-17F (100 ng/mL) for indicated time, the levels of SSeCKS protein in the cytosolic and membrane fraction were determined by Western blotting as described in METHODS ($n = 4$). Representative blots are shown above the bar graphs. $^*P < 0.01$ *versus* control. (Color version of figure is available online.)

In summary, these combined data demonstrate that PKC activation is responsible for IL-17F-induced hyperpermeability, and SSeCKS is an important downstream target of PKC in IL-17F signal pathway in RPMVECs. IL-17F-PKC-SSeCKS axis might be a novel and critical therapeutic target for endothelial barrier dysfunction. Because PKC is a key activator of the cascade at multiple steps and SSeCKS may play critical roles at the junction of PKA and PKC signaling pathways [18, 43, 49], we plan to investigate the PKC–MAPK interaction and the binding of PKC/PKA though SSeCKS in more detail and clarify these questions in IL-17F-induced RPMVECs.

ACKNOWLEDGMENTS

The authors acknowledge funding for this work by grants from the National Science Foundation of China (30670935).

REFERENCES

1. Starnes T, Robertson MJ, Sledge G, et al. Cutting edge: IL-17F, a novel cytokine selectively expressed in activated T cells and monocytes, regulates angiogenesis and endothelial cell cytokine production. J Immunol 2001;167:4137.
2. Kawaguchi M, Onuchic LF, Li XD, et al. Identification of a novel cytokine, ML-1, and its expression in subjects with asthma. J Immunol 2001;167:4430.
3. Kawaguchi M, Kokubu F, Matsukura S, et al. Induction of C-X-C chemokines, growth-related oncogene α expression, and epithelial cell-derived neutrophil-activating protein-78 by ML-1 (interleukin-17F) involves activation of Raf1-mitogen-activated protein kinase kinase-extracellular signal-regulated kinase 1/2 pathway. J Pharmacol Exp Ther 2003;307:1213.
4. Hymowitz SG, Filvaroff EH, Yin JP, et al. IL-17s adopt a cystine knot fold: Structure and activity of a novel cytokine, IL-17F, and implications for receptor binding. EMBO J 2001;20:5332.
5. Wu Q, Martin RJ, Rino JG, et al. IL-23-dependent IL-17 production is essential in neutrophil recruitment and activity in mouse lung defense against respiratory Mycoplasma pneumoniae infection. Microbes Infect 2007;9:78.
6. Tan W, Huang W, Gu X, et al. IL-17F/IL-17R interaction stimulates granulopoiesis in mice. Exp Hematol 2008;36:1417.
7. Happel KI, Dubin PJ, Zheng M, et al. Divergent roles of IL-23 and IL-12 in host defense against Klebsiella pneumoniae. J Exp Med 2005;202:761.
8. Oda N, Canelos PB, Essayan DM, et al. Interleukin-17F induces pulmonary neutrophilia and amplifies antigen-induced allergic response. Am J Respir Crit Care Med 2005;171:12.
9. Sedgwick JB, Menon I, Gern JE, et al. Effects of inflammatory cytokines on the permeability of human lung microvascular endothelial cell monolayers and differential eosinophil transmigration. J Allergy Clin Immunol 2002;110:752.
10. Zhang H, Sun GY. LPS induces permeability injury in lung microvascular endothelium via AT(1) receptor. Arch Biochem Biophys 2005;441:75.
11. Angelini DJ, Hyun SW, Grigoryev DN, et al. TNF-α increases tyrosine phosphorylation of vascular endothelial cadherin and opens the paracellular pathway through fyn activation in human lung endothelia. Am J Physiol Lung Cell Mol Physiol 2006;291:L1232.
12. Numasaki M, Takahashi H, Tomioka Y, et al. Regulatory roles of IL-17 and IL-17F in G-CSF production by lung microvascular endothelial cells stimulated with IL-1β and/or TNF-α. Immunol Lett 2004;95:97.
13. Numasaki M, Tomioka Y, Takahashi H, et al. IL-17 and IL-17F modulate GM-CSF production by lung microvascular endothelial cells stimulated with IL-1β and/or TNF-α. Immunol Lett 2004;95:175.
14. Koss M, Pfeiffer GR. II, Wang Y, et al. Ezrin/radixin/moesin proteins are phosphorylated by TNF-α and modulate permeability increases in human pulmonary microvascular endothelial cells. J Immunol 2006;176:1218.
15. Tinsley JH, Breslin JW, Teasdale NR, et al. PKC-dependent, burn-induced adherens junction reorganization and barrier dysfunction in pulmonary microvascular endothelial cells. Am J Physiol Lung Cell Mol Physiol 2005;289:L217.
16. Tinsley JH, Teasdale NR, Yuan SY. Involvement of PKC δ and PKD in pulmonary microvascular endothelial cell hyperpermeability. Am J Physiol Cell Physiol 2004;286:C105.
17. Brandt D, Gimona M, Hillmann M, et al. Protein kinase C induces actin reorganization *via* a Src- and Rho-dependent pathway. J Biol Chem 2002;277:20903.
18. Corbit KC, Trakul N, Eves EM, et al. Activation of Raf-1 signaling by protein kinase C through a mechanism involving Raf kinase inhibitory protein. J Biol Chem 2003;278:13061.
19. Usatyuk PV, Natarajan V. Role of mitogen-activated protein kinases in 4-hydroxy-2-nonenal-induced actin remodeling and barrier function in endothelial cells. J Biol Chem 2004; 279:11789.
20. Garcia JG, Liu F, Verin AD, et al. Sphingosine 1-phosphate promotes endothelial cell barrier integrity by EGD-dependent cytoskeletal rearrangement. J Clin Invest 2001;108:689.
21. Gelman IH, Tombler E, Vargas J. Jr. A role for SSeCKS, a major protein kinase C substrate with tumor suppressor activity, in cytoskeletal architecture, formation of migratory processes, and cell migration during embryogenesis. Histochem J 2000; 32:13.

22. Gelman IH. The role of SSeCKS/gravin/AKAP12 scaffolding proteins in the spaciotemporal control of signaling pathways in oncogenesis and development. Front Biosci 2002;7:d1782.
23. Lin X, Nelson P, Gelman IH. SSeCKS, a major protein kinase C substrate with tumor suppressor activity, regulates G(1)–>S progression by controlling the expression and cellular compartmentalization of cyclin D. Mol Cell Biol 2000;20:7259.
24. Lin X, Tombler E, Nelson PJ, et al. A novel src- and ras-suppressed protein kinase C substrate associated with cytoskeletal architecture. J Biol Chem 1996;271:28430.
25. Chapline C, Mousseau B, Ramsay K, et al. Identification of a major protein kinase C-binding protein and substrate in rat embryo fibroblasts. Decreased expression in transformed cells. J Biol Chem 1996;271:6417.
26. Gelman IH, Lee K, Tombler E, et al. Control of cytoskeletal architecture by the src-suppressed C kinase substrate, SSeCKS. Cell Motil Cytoskeleton 1998;41:1.
27. Lee SW, Kim WJ, Choi YK, et al. SSeCKS regulates angiogenesis and tight junction formation in blood-brain barrier. Nat Med 2003;9:900.
28. Cheng C, Liu H, Ge H, et al. Lipopolysaccharide induces expression of SSeCKS in rat lung microvascular endothelial cell. Mol Cell Biochem 2007;305:1.
29. Chen SF, Fei X, Li SH. A new simple method for isolation of microvascular endothelial cells avoiding both chemical and mechanical injuries. Microvasc Res 1995;50:119.
30. Zhang H, Sun GY. Expression and regulation of AT1 receptor in rat lung microvascular endothelial cell. J Surg Res 2006; 134:190.
31. Diglio CA, Grammas P, Giacomelli F, et al. Primary culture of rat cerebral microvascular endothelial cells. Isolation, growth, and characterization. Lab Invest 1982;46:554.
32. Laitinen L. Griffonia simplicifolia lectins bind specifically to endothelial cells and some epithelial cells in mouse tissues. Histochem J 1987;19:225.
33. Kelly JJ, Moore TM, Babal P, et al. Pulmonary microvascular and macrovascular endothelial cells: Differential regulation of Ca2+ and permeability. Am J Physiol 1998;274:L810.
34. Chang YS, Munn LL, Hillsley MV, et al. Effect of vascular endothelial growth factor on cultured endothelial cell monolayer transport properties. Microvasc Res 2000;59:265.
35. Jennings LK, Fox JE, Edwards HH, et al. Changes in the cytoskeletal structure of human platelets following thrombin activation. J Biol Chem 1981;256:6927.
36. Stasek JE. Jr., Patterson CE, Garcia JG. Protein kinase C phosphorylates caldesmon77 and vimentin and enhances albumin permeability across cultured bovine pulmonary artery endothelial cell monolayers. J Cell Physiol 1992;153:62.
37. Yang XO, Chang SH, Park H, et al. Regulation of inflammatory responses by IL-17F. J Exp Med 2008;205:1063.
38. Kawaguchi M, Kokubu F, Huang SK, et al. The IL-17F signaling pathway is involved in the induction of IFN-γ-inducible protein 10 in bronchial epithelial cells. J Allergy Clin Immunol 2007; 119:1408.
39. Hizawa N, Kawaguchi M, Huang SK, et al. Role of interleukin-17F in chronic inflammatory and allergic lung disease. Clin Exp Allergy 2006;36:1109.
40. Birukova AA, Adyshev D, Gorshkov B, et al. ALK5 and Smad4 are involved in TGF-β1-induced pulmonary endothelial permeability. FEBS Lett 2005;579:4031.
41. Clements RT, Minnear FL, Singer HA, et al. RhoA and Rho-kinase dependent and independent signals mediate TGF- β-induced pulmonary endothelial cytoskeletal reorganization and permeability. Am J Physiol Lung Cell Mol Physiol 2005; 288:L294.
42. Petrache I, Verin AD, Crow MT, et al. Differential effect of MLC kinase in TNF-α-induced endothelial cell apoptosis and barrier dysfunction. Am J Physiol Lung Cell Mol Physiol 2001; 280:L1168.
43. Nelson PJ, Moissoglu K, Vargas J, Jr., et al. Involvement of the protein kinase C substrate, SSeCKS, in the actin-based stellate morphology of mesangial cells. J Cell Sci 1999;112(Pt 3):361.
44. Kitamura H, Okita K, Fujikura D, et al. Induction of Src-suppressed C kinase substrate (SSeCKS) in vascular endothelial cells by bacterial lipopolysaccharide. J Histochem Cytochem 2002;50:245.
45. Coats SR, Covington JW, Su M, et al. SSeCKS gene expression in vascular smooth muscle cells: Regulation by angiotensin II and a potential role in the regulation of PAI-1 gene expression. J Mol Cell Cardiol 2000;32:2207.
46. Chapline C, Cottom J, Tobin H, et al. A major, transformation-sensitive PKC-binding protein is also a PKC substrate involved in cytoskeletal remodeling. J Biol Chem 1998;273:19482.
47. Nelson PJ, Gelman IH. Cell-cycle regulated expression and serine phosphorylation of the myristylated protein kinase C substrate, SSeCKS: Correlation with culture confluency, cell cycle phase and serum response. Mol Cell Biochem 1997;175:233.
48. Rung-ruangkijkrai T, Fujikura D, Kitamura H, et al. The expression of src-suppressed C kinase substrate (SSeCKS) and uptake of exogenous particles in endothelial and reticular cells. Arch Histol Cytol 2004;67:135.
49. Kolch W, Heidecker G, Kochs G, et al. Protein kinase C α activates RAF-1 by direct phosphorylation. Nature 1993;364:249.